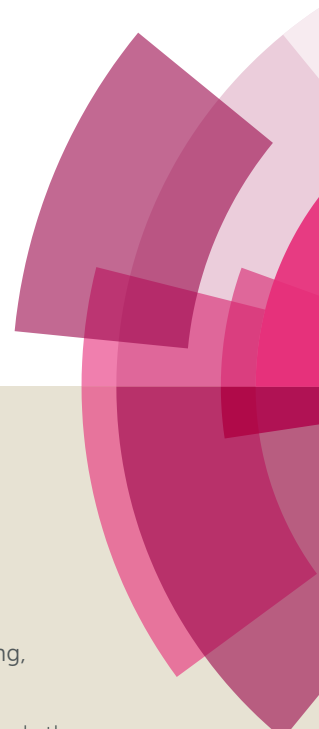


NJC

Accepted Manuscript



This article can be cited before page numbers have been issued, to do this please use: Z. Yang, H. Wang, G. Ji, X. Yu, Y. Chen, X. Liu, C. Wu and Z. Liu, *New J. Chem.*, 2017, DOI: 10.1039/C6NJ03899A.



This is an Accepted Manuscript, which has been through the Royal Society of Chemistry peer review process and has been accepted for publication.

Accepted Manuscripts are published online shortly after acceptance, before technical editing, formatting and proof reading. Using this free service, authors can make their results available to the community, in citable form, before we publish the edited article. We will replace this Accepted Manuscript with the edited and formatted Advance Article as soon as it is available.

You can find more information about Accepted Manuscripts in the [author guidelines](#).

Please note that technical editing may introduce minor changes to the text and/or graphics, which may alter content. The journal's standard [Terms & Conditions](#) and the ethical guidelines, outlined in our [author and reviewer resource centre](#), still apply. In no event shall the Royal Society of Chemistry be held responsible for any errors or omissions in this Accepted Manuscript or any consequences arising from the use of any information it contains.



NJC

COMMUNICATION

Pyridine-functionalized organic porous polymers: applications in efficient CO₂ adsorption and conversion

Received 00th January 20xx,
Accepted 00th January 20xx

Zhenzhen Yang,^a Huan Wang,^{a,b} Guiping Ji,^{a,b} Xiaoxiao Yu,^{a,b} Yu Chen,^{a,b} Xinwei Liu,^{a,b} Cailing Wu,^{a,b} and Zhimin Liu*^{a,b}

DOI: 10.1039/x0xx00000x

www.rsc.org/

Pyridine-functionalized porous organic polymers showed excellent CO₂ uptake capacity (up to 63 and 171 mg g⁻¹ at 0.1 and 1 bar at 273 K), and performed well as good support for Ru(0) nanoparticles. The resultant CarPy-CMP@Ru served as efficient catalyst for the formylation of amines with CO₂/H₂, together with high product yields (89~93%), high stability and easy recyclability.

Compared with conventional inorganic porous materials (e.g., zeolites, silicas and carbon), microporous organic polymers (MOPs) are unique in that they exhibit permanent porosity with extremely high surface areas, and could be prepared via diversified chemical synthetic routes.¹ This provides a wealth of opportunities to control the porous structures as well as frameworks and surface functionalities to cater to the needs of targeted applications. Conjugated microporous polymers (CMPs) are MOPs with π -conjugated skeletons of permanent nanopores and have been widely applied in gas adsorption, photocatalysis, electrical energy storage, heterogeneous catalysis and so on.²

Formamides are a class of chemicals with widespread applications in industry as solvents (e.g. *N,N*-dimethylformamide (DMF)) and raw materials for organic synthesis.³ Industrially, DMF is produced by a NaOCH₃-catalyzed reaction of dimethylamine with toxic CO in methanol.⁴ However, CO is difficult to transport on a bulk scale and its physical properties (especially its toxicity) impede its wider use in academia too. Therefore, carbonylations with cheap, abundant and renewable CO₂ offer a more safe and accessible tool for synthetic organic chemists. An alternative green route for the *N*-formylation of amines is using CO₂ together with H₂ as a formylating reagent. In this respect, efficient homogeneous catalysts based on complexes of Ru,⁵ Fe⁶ and Co⁷ has been developed since 1970. Nevertheless, the

heterogeneous catalysts are more desirable for industrial applications owing to the convenience of recovering and recycling of the catalysts. For example, heterogeneous catalytic system such as SiO₂@Ru,⁸ Cu/ZnO⁹ and HSA-TiO₂-A@Ir¹⁰ was reported for the production of DMF. Shi et al. further extended the substrate scope to various aliphatic utilizing Al₂O₃-NR-RD@Pd catalyst.¹¹

MOPs with nitrogen-rich functionalities such as azo,¹² Tröger's base,¹³ triazine,¹⁴ imidazole¹⁵ and amine¹⁶ showed "CO₂-philic" properties and superior capacity to CO₂ uptake, which is believed to arise from enhanced CO₂-framework interactions. On the other hand, those nitrogen-containing group functionalized MOPs displayed excellent catalytic activities for the chemical conversion of CO₂ into value added chemicals including formic acid,^{13a} methyl amines,¹⁷ organic carbonates¹⁸ and so on. Hence, functionalized MOPs, especially those with high CO₂ adsorption capacities, may exhibit high performance as heterogeneous catalysts for the production of value-added chemicals taking CO₂ as carbonylation feedstock under mild conditions. Although MOPs are quite promising materials for efficient CO₂ (kinetic diameter: 3.3 Å¹⁹) adsorption due to their high microporosity, micropores with small diameters (< 2 nm) are unfavorable for mass transfer, thus limiting the contact of large substrate molecules with the catalytic center within the pores, and the diffusion of the formed product molecules out of the cavities. Therefore, CO₂-philic group functionalized organic polymers materials with hierarchically micro- and mesoporosity will have broad application prospect and favorable for catalytic utilization.

Microporous polycarbazole materials derived from straightforward carbazole-based free radical oxidative coupling polymerization represent a simple synthetic process to obtain CMPs with high BET surface areas (up to 2220 m² g⁻¹ (CPOP-1)).²⁰ Our group has prepared CMPs with tubular morphology using pyridine-containing carbazole, 2,6-di(9H-carbazol-9-yl)pyridine) (CarPy), as monomers via carbazole-based free radical oxidative coupling polymerization catalyzed by FeCl₃ in chloroform (Scheme 1), which was utilized as precursors for *N*-

^a Beijing National Laboratory for Molecular Sciences, Key Laboratory of Colloid, Interface and Thermodynamics, Institute of Chemistry, Chinese Academy of Sciences, Beijing 100190, China. E-mail: liuzm@iccas.ac.cn.

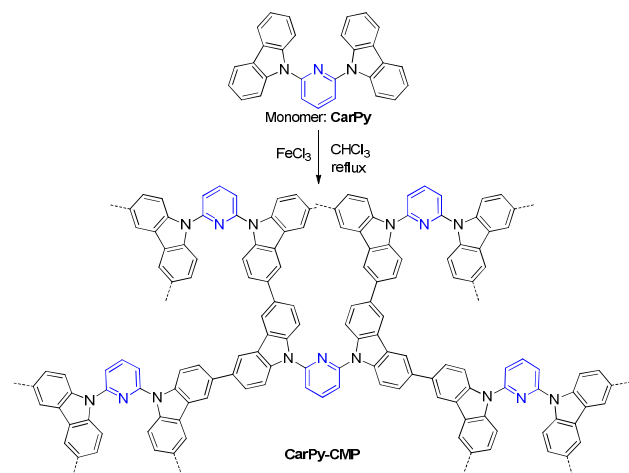
^b University of Chinese Academy of Sciences, Beijing 100049, China
Electronic Supplementary Information (ESI) available: experimental details and additional data and figures. See DOI: 10.1039/x0xx00000x

COMMUNICATION

Journal Name

doped carbon nanotubes.²¹ Notably, the resultant CarPy-CMP exhibited Brunauer–Emmett–Teller (BET) surface area of 993 m² g⁻¹, with both micro- and mesopores existing within the backbone and dominated with mesopore in a volume proportion higher than 75%.²¹ In fact, the application of CarPy-CMP was also explored by Dai's group as a component of frustrated Lewis pairs (FLPs) for ketone hydrogenation. The superior structural and textual properties made it good candidate as heterogeneous catalysts for CO₂ adsorption and conversion, which has not been studied yet.

In this work, CarPy-CMP showed excellent CO₂ uptake capacity (up to 63 and 171 mg g⁻¹ at 0.1 bar and 1 bar at 273 K). Furthermore, the CarPy-CMP supported Ru nanocatalyst (CarPy-CMP@Ru) with a uniform pore size distribution of around 1.7 nm and the hierarchically porous structure served as efficient catalyst for the formylation of amines with CO₂/H₂, together with high product yields (89–93%), high stability and easy recyclability. The excellent performance of CarPy-CMP-1@Ru for CO₂ conversion was ascribed to the joint effect of the polymeric support and the Ru nanoparticles. The polymer served as the support for Ru nanoparticles, meanwhile it could capture CO₂ due to the CO₂-philic nature of pyridine functionality and hierarchically porosity, as well as activate amines through hydrogen bonding formation.



Scheme 1 Synthetic route of pyridine-derived CMP networks CarPy-CMP.

Firstly, the prepared pyridine-functionalized polycarbazole CMPs (CarPy-CMP) were detected for CO₂ uptake. It was demonstrated that the CO₂ adsorption/desorption isotherms were completely reversible at 273 K, indicating that the interactions between CO₂ and the backbone of the polymers was weak enough to allow CO₂ desorption without heating (Figure 1a). The surface functionality of the sorbents with pyridine had a significant effect in the low-pressure regime, where the adsorption capacity was mainly dependent on the CO₂-sorbent interactions, other than the surface area.²² For example, the CO₂ adsorption capacity of CarPy-CMP was 63 mg g⁻¹ at 0.1 bar and 273 K, which was higher than those of the other carbazole-derived CMPs with higher BET surface areas (e.g. ~20 mg g⁻¹ for CPOP-7 with BET surface area of 1430 m² g⁻¹

¹)²³. The superiority of pyridine-functionalized CarPy-CMP was also pronounced at 1 bar and 273 K (171 mg g⁻¹), much better than the reported carbazole-derived CMPs such as CPOP-7 under the same conditions (for comparison of CO₂ adsorption capacities with other CMPs derived from carbazole monomers, see Table S1, ESI).⁹ Comparatively, CO₂ capacity of ~90 mg g⁻¹ (1 bar) and 16 mg g⁻¹ (0.1 bar) for CarPy-CMP was obtained at 298 K. The CO₂-philic nature of the pyridine-functionalized polymers was also indicated by the higher CO₂ isosteric heat of adsorption (Q_{st}) values of 35.0 kJ mol⁻¹ compared with the values of most of the CMP materials (Figure 1b), which were within the desirable range for CO₂ sorbents.²⁴

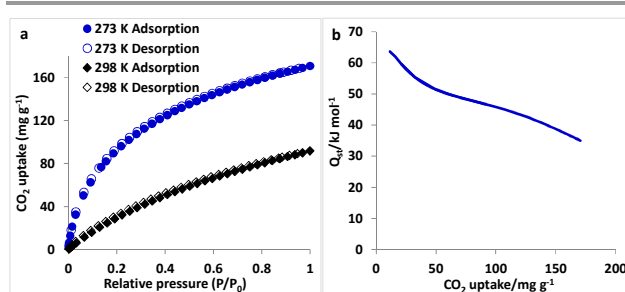


Figure 1 a) CO₂ adsorption (filled) and desorption (empty) isotherms measured for CarPy-CMP at 273 K and 298 K. b) Isosteric heats of adsorption (Q_{st}) for CO₂. Isosteric heats of adsorption were calculated from the adsorption data at 273 and 298 K using Clausius-Clapeyron equation.

As stated above, pyridine-functionalized CMP nanotubes were good sorbents for CO₂ capture, and the hierarchically porous nature maybe makes them good catalyst candidates for the subsequent chemical conversion of CO₂. CarPy-CMP supported Ru nanocatalyst (CarPy-CMP@Ru) was prepared through reductive deposition (for experimental details, see ESI). It was indicated that the Ru nanoparticles (NPs) were uniformly distribution on the surface of the nanotubes, and the particle sizes were centered around 1.7 nm observed by (HR)TEM (Figure S1, ESI). CarPy-CMP-1@Ru was further characterized by energy dispersive spectrometer (EDS) profile (Figure S2d, ESI), which indicated the existence of mainly Ru, C, N within the material (trace amount of O, Cu and Si were induced by lacey support films). X-ray photoelectron spectroscopy (XPS) spectra (Figure S2a-c, ESI) indicated that the Ru species were mainly in the metallic form with binding energy (BE) at 281.2 eV for Ru(0)3d_{5/2}, shifting to higher values compared to those of the bulk Ru (280.0 eV),²⁵ suggesting the strong interaction between the Ru nanoparticles and the support. Compared with the BEs of Ru3p_{3/2} and Ru3p_{1/2} in Ru(III) (463.73 and 486.08 eV),¹⁷ those in CarPy-CMP@Ru decreased to 462.77 and 484.77 eV, which also confirmed the existence of Ru(0) NPs. To testify the coordination of Ru(0) NPs with the polymer network, the BEs of C1s and N1s was investigated. As shown in Figure S2a in ESI, the BEs of C1s was increased from 284.72 and 285.87 eV (CarPy-CMP) to 284.77 and 286.02 eV (CarPy-CMP@Ru) after Ru(0) NPs coordination.²¹ Simultaneously, the increase of BEs for N1s was also observed, from 399.27 and 399.92 eV (CarPy-CMP) to 399.47 and 400.27 eV (CarPy-CMP@Ru) (Figure S2b, ESI). All

these results confirmed the strong coordination of Ru(0) with the polymer backbone, hence indicating the significant stability of the supported Ru(0) NPs, probably owing to the rough surface of the polymer nanotubes and also abundant nitrogen group-containing functionalities. The Ru content determined by inductively coupled plasma-optical emission spectroscopy (ICP-OES) analysis for **Car-CMP-1@Ru** was 2.47 wt%.

The textual information on **CarPy-CMP@Ru** was obtained by N₂ sorption analysis at 77 K. The obtained N₂ physisorption isotherms exhibited combined features of type I and type II with two obviously steep steps in the regions of P/P₀ < 0.01 and 0.80 < P/P₀ < 0.98, suggesting the coexistence of micro- and mesopores (Figure 2). Based on the calculation results of the nonlocal density functional theory method (NLDFT), micropores with mean size at 0.5 nm and mesopores with pore diameter in the range of 2~35 nm were present. Moreover, the BET surface area of **CarPy-CMP@Ru** reached 735.7 m² g⁻¹ (Figure S3), slightly lower than that of CarPy-CMP (993 m² g⁻¹) due to introduction of Ru(0) NPs. Its pore volume was dominated with mesopore in a volume proportion of 81%, with total pore volume of 1.02 cm³ g⁻¹ (at P/P₀ = 0.99) and micropore volume of 0.19 cm³ g⁻¹ (at P/P₀ = 0.2~0.4). Therefore, the hierarchically porous structure of **CarPy-CMP@Ru** would be favorable for mass transfer in heterogeneous catalysis.

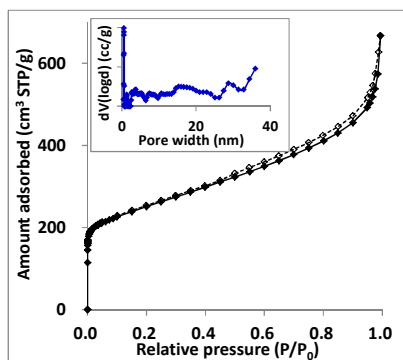


Figure 2 Adsorption (filled) and desorption (empty) isotherms of N₂ at 77 k for **CarPy-CMP@Ru**. The inset was the pore size distributions based on the calculation results of the NLDFT method.

Subsequently, **Car-CMP-1@Ru** was applied in catalyzing the formylation of amines with CO₂/H₂. Formylation of morpholine (**1a**) was taken as the model reaction to optimize the reaction conditions (Table 1). Excitingly, **Car-CMP-1@Ru** was found to be very effective for this reaction, affording 94% yield of N-formylmorpholine (**2a**), much better than the commercially available Ru/C (**2a** yield: 29%) (Table 1, entry 1 vs 2). Trace amount of 4-methylmorpholine (**3a**) was detected as byproduct, being produced by further reduction of **2a**. Other solvents such as ethanol, acetonitrile and 1,4-dioxane showed inferior performance, with 43~64% yield of **2a** being achieved (entries 3~5). The reaction was very sensitive to temperature, and the yield of **2a** was sharply decreased to 47% at 120 °C (entry 6). If the catalyst loading was further decreased to 0.25

mol%, 68% yield of **2a** was still obtained within 24 h (entry 7). In addition, further effort to decreased to pressure of CO₂/H₂ resulted in lower catalytic activities (entries 8 and 9). The excellent performance of **Car-CMP-1@Ru** for CO₂ conversion was ascribed to the joint effect of the polymeric support and the Ru nanoparticles. The polymer served as the support for Ru nanoparticles, meanwhile it could capture CO₂ due to the CO₂-philic nature of pyridine functionality and hierarchically porosity. Notably, the supported Ru(0) NPs was essentially important for the activation of H₂ as well as the subsequent CO₂ reduction during the amine formylation process.⁹⁻¹¹ As shown in Table 1 (entry 10), no reaction occurred using solely polymer (**CarPy-CMP**) as catalyst under the same reaction conditions.

In addition, activation of morpholine through hydrogen bonding with the pyridine among the skeleton maybe also facilitated the reaction process, as detected by NMR spectra (Figure S4, ESI). It was found that the proton of morpholine showed a downfield shift from 2.82 and 3.62 ppm to 2.88 and 3.69 ppm in the ¹H NMR spectra, and correspondingly, similar phenomena was observed in the ¹³C NMR spectra, with the carbon signal of morpholine shifted from 44.9 and 66.3 ppm to 46.5 and 68.1 ppm, respectively.

Table 1 Formylation of piperazine with CO₂ and H₂ catalyzed by **Car-CMP-1@Ru**^a

Entry	Solvent	1a Conv./% ^b	2a Yield/% ^b	3a Yield/% ^b
1	MeOH	97	94	<1
2 ^c	MeOH	33	29	<1
3	EtOH	67	64	<1
4	CH ₃ CN	66	57	3
5	1,4-Dioxane	51	43	4
6 ^d	MeOH	50	47	1
7 ^e	MeOH	77	68	4
8 ^f	MeOH	81	78	<1
9 ^g	MeOH	40	33	<1
10 ^h	MeOH	<1	0	0

^a Reaction conditions: **1a** 1 mmol, catalyst loading 0.5 mol% based on **1a**, CO₂ 4 MPa, total pressure of CO₂ and H₂ 8 MPa, solvent 3 mL, 130 °C, 24 h. ^b Determined by GC using dodecane as an internal standard. ^c Using commercialized Ru/C (5 wt%) as catalyst. ^d 120 °C. ^e catalyst loading 0.25 mol%. ^f CO₂ 3 MPa, total pressure of CO₂ and H₂ 6 MPa. ^g CO₂ 2 MPa, total pressure of CO₂ and H₂ 4 MPa. ^h 20 mg **CarPy-CMP** was added as catalyst.

Most importantly, the catalyst **CarPy-CMP@Ru** showed good reusability and easy recyclability through filtration, confirmed by the fact that 91% yield of **2a** was still obtained after the catalyst was reused five times (Figure S5a, ESI). The TEM images indicated no aggregation of Ru(0) nanoparticles, primarily owing to stabilization of the metal species by the electron-donating functionalities (carbazole and pyridine) among the backbone of the CMP (Figure S5b, ESI). In addition, there was no Ru species detected in the filtrate of the reaction mixture by ICP-OES, indicating the strong coordination ability

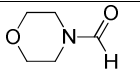
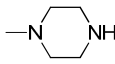
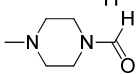
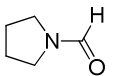
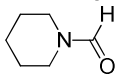
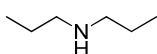
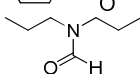
COMMUNICATION

Journal Name

of Ru species with the polymeric framework and the good stability of **CarPy-CMP@Ru** as an efficient heterogeneous catalyst.

Other cyclic secondary amines such as 4-methylpiperidine, pyrrolidine and piperidine were also converted into the corresponding formamides in the presence of CO₂/H₂ with 90~93% yields under the optimized conditions (Table 2, entries 2~4). Other dialkylamine, such as dipropylamine, led to the formylation product in 89% yield (entry 5).

Table 2 Formylation of amines catalyzed by Car-CMP-1@Ru in the presence of CO₂/H₂^a

Entry	Substrates	Products	Yields/% ^b
1			91
2			93
3			90
4			93
5			89

^a Reaction conditions: amine 1 mmol, catalyst loading 0.5 mol% Ru based on amine, MeOH 3 mL, CO₂ pressure 4 MPa, total pressure (CO₂ + H₂) 8 MPa, 130 °C, 24 h. ^b Isolated yield.

Pyridine-functionalized porous organic polymers showed excellent CO₂ uptake capacity as well as good support for Ru(O) nanoparticles. The supported Ru nanocatalyst with uniform pore size distribution and the hierarchically porous structure served as efficient catalyst for the formylation of amines with CO₂/H₂, together with high product yields, high stability and easy recyclability. Its excellent performance for CO₂ conversion was ascribed to the joint effect of the polymeric support and the Ru nanoparticles. The polymer served as the support for Ru nanoparticles, meanwhile it could capture CO₂ due to the CO₂-philic nature of pyridine functionality and hierarchically porosity, as well as activate amines through hydrogen bonding formation.

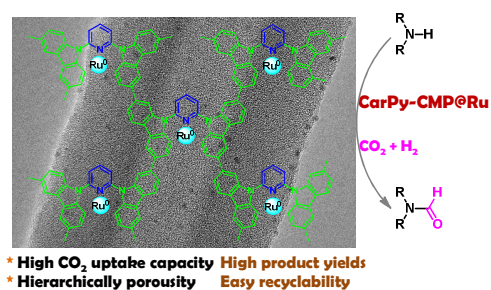
Acknowledgements

This work was financially supported by the National Natural Science Foundation of China (grant no. 21402208, 21533011, 21125314).

Notes and references

- 1 a) D. Wu, F. Xu, B. Sun, R. Fu, H. He and K. Matyjaszewski, *Chem. Rev.*, 2012, **112**, 3959-4015; b) C. Perego and R. Millini, *Chem. Soc. Rev.*, 2013, **42**, 3956-3976.
- 2 a) Y. Xu, S. Jin, H. Xu, A. Nagai and D. Jiang, *Chem. Soc. Rev.*, 2013, **42**, 8012-8031; b) F. Vilela, K. Zhang and M. Antonietti, *Energy Environ. Sci.*, 2012, **5**, 7819-7832; c) S. Bhunia, B. Banerjee and A. Bhaumik, *Chem. Commun.*, 2015, **51**, 5020-

- 5023; d) S. Mondal, J. Mondal and A. Bhaumik, *ChemCatChem*, 2015, **7**, 3570-3578.
- 3 K. Weissert and H.-J. Arpe, in *Industrial Organic Chemistry, 3rd ed.*, Translated by C. R. Lindley, Wiley-VCH, Weinheim, 1997.
- 4 H. Bipp and H. Kieczka, in *Ullmann's Encyclopedia of Industrial Chemistry*, Wiley-VCH, Weinheim, 2000.
- 5 L. Zhang, Z. Han, X. Zhao, Z. Wang and K. Ding, *Angew. Chem. Int. Ed.*, 2015, **54**, 6186-6189.
- 6 C. Ziebart, C. Federsel, P. Anbarasan, R. Jackstell, W. Baumann, A. Spannenberg and M. Beller, *J. Am. Chem. Soc.*, 2012, **134**, 20701-20704.
- 7 C. Federsel, C. Ziebart, R. Jackstell, W. Baumann and M. Beller, *Chem. Eur. J.*, 2012, **18**, 72-75.
- 8 O. Kröcher, R. A. Köppel, M. Fröba and A. Baiker, *J. Catal.*, 1998, **178**, 284-298.
- 9 J. Liu, C. Guo, Z. Zhang, T. Jiang, H. Liu, J. Song, H. Fan and B. Han, *Chem. Commun.*, 2010, **46**, 5770-5772.
- 10 Q.-Y. Bi, J.-D. Lin, Y.-M. Liu, S.-H. Xie, H.-Y. He and Y. Cao, *Chem. Commun.*, 2014, **50**, 9138-9140.
- 11 X. Cui, Y. Zhang, Y. Deng and F. Shi, *Chem. Commun.*, 2014, **50**, 189-191.
- 12 a) H. A. Patel, S. Hyun Je, J. Park, D. P. Chen, Y. Jung, C. T. Yavuz and A. Coskun, *Nat. Commun.*, 2013, **4**, 1357; b) G. Ji, Z. Yang, H. Zhang, Y. Zhao, B. Yu, Z. Ma and Z. Liu, *Angew. Chem. Int. Ed.*, 2016, **55**, 9685-9689.
- 13 a) Z.-Z. Yang, H. Zhang, B. Yu, Y. Zhao, G. Ji and Z. Liu, *Chem. Commun.*, 2015, **51**, 1271-1274; b) X. Zhu, C.-L. Do-Thanh, C. R. Murdock, K. M. Nelson, C. Tian, S. Brown, S. M. Mahurin, D. M. Jenkins, J. Hu, B. Zhao, H. Liu and S. Dai, *ACS Macro Lett.*, 2013, **2**, 660-663; c) Z. G. Wang, X. Liu, D. Wang and J. Jin, *Polym. Chem.*, 2014, **5**, 2793-2800.
- 14 a) A. Thomas, *Angew. Chem. Int. Ed.*, 2010, **49**, 8328-8344; b) X. Zhu, C. Tian, G. M. Veith, C. W. Abney, J. Dehaut and S. Dai, *J. Am. Chem. Soc.*, 2016, **138**, 11497-11500.
- 15 a) M. G. Rabbani and H. M. El-Kaderi, *Chem. Mater.*, 2011, **23**, 1650-1653; b) R. Ullah, M. Atilhan, A. Diab, E. Deniz, S. Aparicio and C. T. Yavuz, *Adsorption*, 2016, **22**, 247-260; c) A. K. Sekizkardes, S. Altarawneh, Z. Kahveci, T. İslamoğlu and H. M. El-Kaderi, *Macromolecules*, 2014, **47**, 8328-8334.
- 16 R. Dawson, E. Stockel, J. R. Holst, D. J. Adams and A. I. Cooper, *Energy Environ. Sci.*, 2011, **4**, 4239-4245.
- 17 Z. Yang, H. Zhang, B. Yu, Y. Zhao, Z. Ma, G. Ji, B. Han and Z. Liu, *Chem. Commun.*, 2015, **51**, 11576-11579.
- 18 Y. Xie, T.-T. Wang, X.-H. Liu, K. Zou and W.-Q. Deng, *Nat. Commun.*, 2013, **4**, 1960.
- 19 D. M. D'Alessandro, B. Smit and J. R. Long, *Angew. Chem. Int. Ed.*, 2010, **49**, 6058-6082.
- 20 Q. Chen, M. Luo, P. Hammershøj, D. Zhou, Y. Han, B. W. Laursen, C.-G. Yan and B.-H. Han, *J. Am. Chem. Soc.*, 2012, **134**, 6084-6087.
- 21 Z. Yang, Z. Liu, H. Zhang, B. Yu, Y. Zhao, H. Wang, G. Ji, Y. Chen, X. Liu and Z. Liu, *Chem. Commun.*, 2017, 10.1039/C1036CC09374D.
- 22 Y. Zhao, K. X. Yao, B. Teng, T. Zhang and Y. Han, *Energy Environ. Sci.*, 2013, **6**, 3684-3692.
- 23 Q. Chen, D.-P. Liu, M. Luo, L.-J. Feng, Y.-C. Zhao and B.-H. Han, *Small*, 2014, **10**, 308-315.
- 24 C. E. Wilmer, O. K. Farha, Y.-S. Bae, J. T. Hupp and R. Q. Snurr, *Energy Environ. Sci.*, 2012, **5**, 9849-9856.
- 25 P. Zhang, T. Wu, T. Jiang, W. Wang, H. Liu, H. Fan, Z. Zhang and B. Han, *Green Chem.*, 2013, **15**, 152-159.



Pyridine-functionalized porous organic polymers showed excellent CO₂ uptake capacity and served as efficient catalyst for the formylation of amines with CO₂/H₂ after metallization with Ru(0) nanoparticles.